

Convenient Entry to Mono- and Dinuclear Palladium(II) Benzothiazolin-2-ylidene Complexes and Their Activities toward Heck Coupling

Swee Kuan Yen,[†] Lip Lin Koh,[†] F. Ekkehardt Hahn,[‡] Han Vinh Huynh,^{*,†} and T. S. Andy Hor^{*,†}

Department of Chemistry, National University of Singapore, 3 Science Drive 3, Kent Ridge, Singapore 117543, and Institut für Anorganische und Analytische Chemie der Westfälischen Wilhelms-Universität Münster, Corrensstrasse 36, D-48149 Münster, Germany

Received June 9, 2006

Under solventless conditions, benzothiazole reacts with benzyl bromide to give near-quantitative yield of the salt *N*-benzylbenzothiazolium bromide (**A**), which is a convenient air-stable heterocyclic carbene precursor. Treatment of **A** with Pd(OAc)₂ in CH₃CN affords the bis(carbene) complex *cis*-[PdBr₂(NHC)₂] (**1**) (NHC = *N*-benzylbenzothiazolin-2-ylidene). In DMSO, this reaction yields an unprecedented dinuclear N,S-heterocyclic carbene complex, [PdBr₂(NHC)₂] (**2**). Complex **2** undergoes bridge cleavage reactions with CH₃CN and DMF to give the mononuclear and solvated monocarbene complexes *trans*-[PdBr₂(NHC)(Solv)] [Solv = CH₃CN (**3**) and DMF (**4**)]. All compounds have been fully characterized by ¹H and ¹³C NMR spectroscopy, ESI or FAB mass spectrometry, and elemental analysis. The molecular structures of **A** and **1–4** have been determined by X-ray single-crystal diffraction. The catalytic activities of **1–4** toward Mizoroki–Heck coupling reactions of aryl bromides with *tert*-butyl acrylate are described and compared.

Introduction

The discovery of the first stable nucleophilic N-heterocyclic carbene (NHC) in 1991¹ was quickly followed by a plethora of activities on a range of NHCs with strong σ -donating but negligible π -accepting characters.² These ligands can stabilize metals in different oxidation states and support catalytically active intermediates that are coordinatively unsaturated.³ Due to their strong donor ability, they are often considered as alternatives to the much more widespread tertiary phosphines, since the latter often comes with problems such as facile dissociation, low thermal tolerance, high toxicity, and, in some cases, pyrophoricity and susceptibility to oxidation or hydrolysis. Particularly, NHCs derived from imidazole, imidazoline, and, to a lesser extent, benzimidazole have been successfully employed as ancillary ligands in catalysis.⁴ These commonly contain an N,N-heterocyclic ring, whereas NHCs with other heterocyclic rings (such as N,S) are much less developed. Accordingly, the catalytic effects brought about by a more electropositive and softer sulfur as opposed to nitrogen are much less clear. Early work by Breslow⁵ described the application of N,S-heterocyclic carbenes as organo-catalysts such as the vitamin B₁ catalyzed benzoin condensation reactions. Transition metal complexes of N,S-heterocyclic carbenes can be obtained

via metal insertion into the electron-rich olefin 3,3'-dimethyl-2,2'-bibenzothiazolinyliidene or by oxidative addition of 2-chloro-substituted thiazolium salts in low-valent metal precursors as reported by Lappert⁶ and Stone,⁷ respectively. The air-sensitivity of free N,S-heterocyclic carbenes and their high tendency to form electron-rich dimers limited the study of their coordination chemistry, until Raubenheimer⁸ reported a new pathway for N,S-heterocyclic carbene complexes by transmetalation of lithiated thiazoles in 1985. Recently, we reported the preparation of benzothiazolin-2-ylidene complexes of Ir(I) by in situ deprotonation of benzothiazolium salts.⁹ Surprisingly perhaps, the catalytic chemistry of only one N,S-heterocyclic carbene complex has been investigated in detail by Calò and co-workers, who described a straightforward synthesis of a *trans*-bis(carbene) Pd(II) complex by in situ deprotonation of *N*-methylbenzothiazolium iodide with Pd(OAc)₂ and its catalytic activity in various

* Corresponding authors. E-mail: chmhhv@nus.edu.sg (H.V.H.); andyhor@nus.edu.sg (T.S.A.H.).

[†] National University of Singapore.

[‡] Westfälischen Wilhelms-Universität Münster.

(1) Arduengo, A. J., III; Harlow, R. L.; Kline, M. *J. Am. Chem. Soc.* **1991**, *113*, 361.

(2) For reviews see: (a) Herrmann, W. A.; Köcher, C. *Angew. Chem., Int. Ed. Engl.* **1997**, *36*, 2162. (b) Bourissou, D.; Guerret, O.; Gabbai, F. P.; Bertrand, G. *Chem. Rev.* **2000**, *100*, 39. (c) Jafarpour, Z.; Nolan, S. P. *Adv. Organomet. Chem.* **2001**, *46*, 181. (d) Hahn, F. E. *Angew. Chem., Int. Ed.* **2006**, *45*, 1348.

(3) For review see: Herrmann, W. A. *Angew. Chem., Int. Ed.* **2002**, *41*, 1290.

(4) (a) Huang, J. K.; Stevens, E. D.; Nolan, S. P.; Petersen, J. L. *J. Am. Chem. Soc.* **1999**, *121*, 2674. (b) Scholl, M.; Trnka, T. M.; Morgan, J. P.; Grubbs, R. H. *Tetrahedron Lett.* **1999**, *40*, 2247. (c) Stauffer, S. R.; Lee, S. W.; Stambuli, J. P.; Hauck, S. I.; Hartwig, J. F. *Org. Lett.* **2000**, *2*, 1423. (d) Loch, J. A.; Albrecht, M.; Peris, E.; Mata, J.; Faller, J. W.; Crabtree, R. H. *Organometallics* **2000**, *21*, 700. (e) Perry, M. C.; Cui, X. H.; Powell, M. T.; Hou, D. R.; Reibenspies, J. H.; Burgess, K. *J. Am. Chem. Soc.* **2003**, *125*, 113. (f) Miecznikowski, J. R.; Crabtree, R. H. *Organometallics* **2004**, *23*, 629. (g) Muehlhofer, M.; Strassner, T.; Hermann, W. A. *Angew. Chem., Int. Ed.* **2002**, *41*, 1745. (h) Huynh, H. V.; Neo, T. C.; Tan, G. K. *Organometallics* **2006**, *25*, 1298.

(5) Breslow, R. *J. Am. Chem. Soc.* **1958**, *80*, 3719.

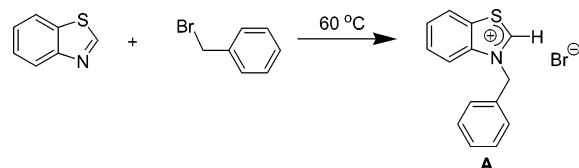
(6) (a) Cardin, D. J.; Cetinkaya, B.; Cetinkaya, E.; Lappert, M. F. *J. Chem. Soc., Dalton Trans.* **1972**, *2*, 1983. (b) Cetinkaya, B.; Dixneuf, P.; Lappert, M. F. *J. Chem. Soc., Dalton Trans.* **1974**, *4*, 226.

(7) Fraser, P. J.; Roper, W. R.; Stone, F. G. A. *J. Chem. Soc., Dalton Trans.* **1973**, *3*, 1129.

(8) For review see: (a) Raubenheimer, H. G.; Cronje, S. *J. Organomet. Chem.* **2001**, *617–618*, 170. (b) Raubenheimer, H. G.; Toit, A. d.; Toit, M. d.; An, J.; Niekerk, L. v.; Cronje, S.; Esterhuysen, C.; Crouch, A. M. *Dalton Trans.* **2004**, 1173.

(9) Huynh, H. V.; Meier, N.; Pape, T.; Hahn, F. E. *Organometallics* **2006**, *25*, 3012.

Scheme 1. Synthesis of Benzothiazolium Salt A



organic transformations.¹⁰ In relation to our recent studies in phosphine- and imine-based catalysts,¹¹ we herein turn our attention to explore the potential of N,S-heterocyclic carbenes as phosphine mimics in catalysis. Reported here is the successful use of *N*-benzylbenzothiazolium salt as a direct entry to N,S-heterocyclic carbenes and the use of the resultant novel monomeric and dimeric benzothiazolin-2-ylidene complexes as catalysts for Mizoroki–Heck reactions.

Results and Discussion

Solvent-Free Synthesis of Benzothiazolium Salt A. *N*-Benzylbenzothiazolium bromide (A) can be obtained in 65% yield from a reaction of benzothiazole with benzyl bromide in DMF at 95 °C.¹² However, the moderate yield and the need to use dry and high-boiling DMF as solvent prompted us to seek a simpler and more convenient method. We could not obtain significant yields of A in a range of alternative solvents. However, when neat benzothiazole is treated with benzyl bromide in the absence of a solvent at 60 °C (Scheme 1), the desired product A readily precipitates from the liquid mixture, which solidifies toward the end of the reaction. Washing with Et₂O gives pure A as an off-white powder in quantitative yield.

The ¹H NMR spectrum of A shows a characteristic downfield resonance at 12.27 ppm for the SCHN proton, indicating the formation of an azolium salt. The formation of A is also supported by a signal at 165.1 ppm in the ¹³C NMR spectrum for the SCN carbon and a base peak at *m/z* = 226 for the azolium cation in the positive mode ESI mass spectrum. The identity of A was further confirmed by its molecular structure (Figure 1) elucidated by single-crystal X-ray diffraction.

Direct Entry to Palladium(II) N,S-Heterocyclic Carbene Complexes. The convenient and high-yield synthesis of *N*-benzylbenzothiazolium bromide A paved an attractive route to enter directly into the N,S-heterocyclic carbene complexes of Pd(II) in a one-pot synthesis. This is based on the methodology developed for Pd(II) dicarbene complexes by using in situ deprotonation of azolium salts with basic metal precursors.^{13–16} Calò et al. used a similar strategy to prepare a Pd(II) bis-(benzothiazolin-2-ylidene) complex from *N*-methylbenzothiazolium iodide and Pd(OAc)₂ in THF.^{10a} Accordingly, we have prepared stable orange solids of the bis(N,S-carbene) complex *cis*-[PdBr₂(NHC)₂] (1) in good yield (91%) from Pd(OAc)₂ and 2 equiv of A in refluxing CH₃CN (Scheme 2). The positive mode ESI mass spectrum is dominated by an isotopic pattern

(10) (a) Calò, V.; Del Sole, R.; Nacci, A.; Schingaro, E.; Scorgari, F. *Eur. J. Org. Chem.* **2000**, 869. (b) Calò, V.; Nacci, A.; Lopez, L.; Mannarini, N. *Tetrahedron Lett.* **2000**, 41, 8973. (c) Calò, V.; Nacci, A.; Lopez, L.; Napola, A. *Tetrahedron Lett.* **2001**, 42, 4701. (d) Calò, V.; Nacci, A.; Monopoli, A.; Lopez, L.; Cosmo, A. *d. Tetrahedron* **2001**, 57, 6071. (e) Calò, V.; Giannoccaro, P.; Nacci, A.; Monopoli, A. *J. Organomet. Chem.* **2002**, 645, 152. (f) Calò, V.; Nacci, A.; Monopoli, A.; Spinelli, M. *Eur. J. Org. Chem.* **2003**, 8, 1382.

(11) (a) Weng, Z. Q.; Teo, S.; Koh, L. L.; Hor, T. S. A. *Chem. Commun.* **2006**, 12, 1319. (b) Teo, S.; Weng, Z. Q.; Hor, T. S. A. *Organometallics* **2006**, 25, 1199. (c) Weng, Z. Q.; Teo, S.; Koh, L. L.; Hor, T. S. A. *Angew. Chem., Int. Ed.* **2005**, 44, 7560.

(12) Baldwin, J. E.; Branz, S. E.; Walker, J. A. *J. Org. Chem.* **1977**, 42, 4143.

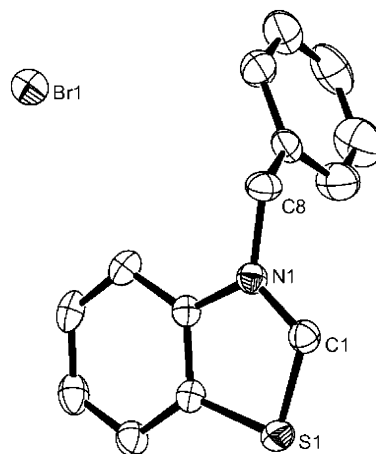
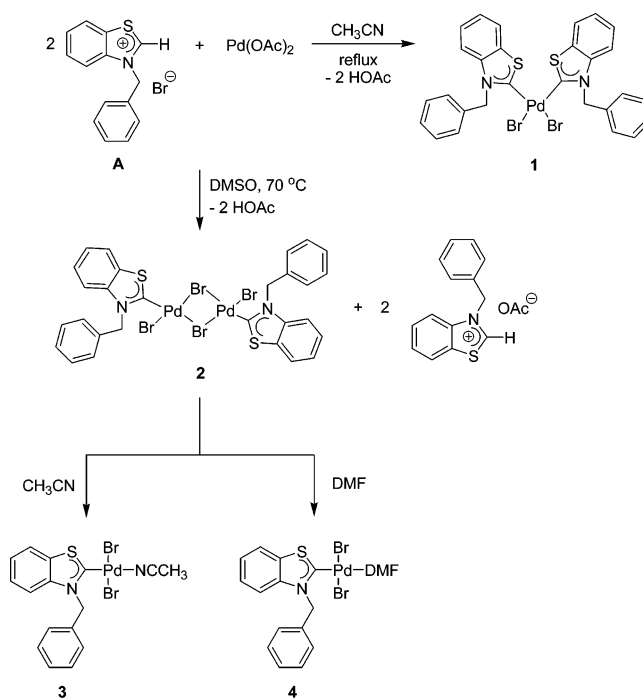


Figure 1. Molecular structure of benzothiazolium salt C₁₄H₁₂BrNS (A) with 50% thermal ellipsoids and labeling scheme; hydrogen atoms are omitted for clarity.

Scheme 2. Synthesis of Palladium(II) Carbene Complexes 1–4



centered at *m/z* = 637 corresponding to a monocation formed upon bromide dissociation from 1. At ambient temperature, the ¹H NMR spectrum (DMSO-*d*₆) of 1 exhibits broad signals that are slightly shifted upfield from the values observed for the benzothiazolium salt A. One broad singlet is noted at 6.34 ppm for both methylene groups, indicating a relatively high energy barrier for the rotation around the Pd–C bond arising from the bulky benzyl substituent on the carbene ligand. The ¹³C carbenoid resonance at 203.8 ppm is significantly more upfield than the analogous resonance observed by Calò et al. in their *trans*-complex (210.5 ppm),^{10a} which points to a *cis*-configuration of the carbene ligands in 1. The identity of 1 has been established, although its carbon analyses in elemental analysis remains unsatisfactory due to some solvent lattice contained in the molecule. Surprisingly, when the reaction is carried out in DMSO at 70 °C, a bromo-bridged dinuclear Pd(II) complex, [PdBr₂(NHC)₂] (2), forms, which shows a 1:1 carbene-to-metal ratio. The absence of the downfield signal for the SCHN proton in the ¹H NMR spectrum indicates a successful complexation.

Although the carbene resonance could not be detected in the ^{13}C NMR spectrum, the FAB mass spectrometric data also point to a dinuclear skeletal structure ($m/z = 903$ corresponding to $[2 - \text{Br}]^+$). To the best of our knowledge, complex **2** is the first example of a dinuclear complex incorporating N,S-heterocyclic carbene ligands. These results also suggest that the formation of mono- versus dicarbene complexes is driven more by the solvent rather than substrate stoichiometry.

The solvent has an additional effect on the dinuclear product. In the presence of donating solvents such as CH_3CN or DMF, bridge cleavage readily occurs, giving the mononuclear solvato complexes *trans*-[PdBr₂(NHC)(CH₃CN)] (**3**) and *trans*-[PdBr₂(NHC)(DMF)] (**4**), as shown in Scheme 2. A different solvent effect that influences the formation of geometric isomers has been reported for related bis(carbene) palladium(II) complexes.¹⁷ The ^{13}C carbenoid signals of **3** and **4** occur at 191.0 and 191.9 ppm, respectively.

Molecular Structures of Complexes 1–4. The molecular structures of complexes **1–4** have been determined by X-ray single-crystal diffraction studies. Selected bond lengths and bond angles are compared to those of salt **A** and summarized in Table 1.

The structure determination of complex **1** reveals an essentially mononuclear square-planar Pd(II) coordinated by two NHCs and two bromo ligands in a *cis*-arrangement (Figure 2).

The NHC planes are oriented nearly perpendicularly to the PdC₂Br₂ coordination planes with dihedral angles of 71.2° and 77.5° as a means to minimize interligand interactions between the carbenes. The Pd–C bond distances (1.971(5) and 1.976(4) Å) are notably shorter than those found in *trans*-diiodobis-(*N*-methylbenzothiazolin-2-ylidene)palladium(II) (2.06(3) Å),^{10a} suggesting a stronger Pd–C bond in *cis*-complexes. These bonds are also shorter than those found in a *cis*-dibromobis(benzimidazolin-2-ylidene)palladium(II) complex (1.996 Å).¹⁸ The other complexes studied herein have even shorter, and presumably stronger, Pd–C bonds. The Pd–Br bond lengths (2.4701(5) Å), on the other hand, are comparable to other *cis*-dibromobis(carbene) complexes of palladium(II).¹⁸ The N(1)–C(1)–S(1) angle of the ligand precursor **A** (114.14°) has contracted to 110.9° upon coordination to give **1**. Other structural parameters remain largely unchanged, indicating that the coordination to the Pd center mainly affects the carbene carbon and the neighboring nitrogen and sulfur atoms.

The dimeric molecular structure of the CHCl_3 solvate of **2** was also confirmed by an X-ray single-crystal diffraction study (Figure 3). Each of the two Pd(II) centers is coordinated by one carbene, one terminal bromo, and two bridging μ -bromo ligands in an almost perfect square-planar fashion.

The metal, which is formally in electron-insufficient condition, can be stabilized by the basic bridging bromide. This is an important consideration for catalyst stabilization under conditions in which the carbene concentration is kept low to avoid oversaturating the metal. The two carbene ligands in **2** are *anti* to each other across the flat dinuclear frame. The dihedral angles between both carbene ring planes and the coordination plane amount to 68.8° and 74.7°, respectively.

Surprisingly, both *N*-benzyl substituents are on the same side of the metal coordination plane. The Pd–C bonds (1.936(7) and 1.960(8) Å) are even shorter and stronger than those in **1**, again indicating higher Lewis acidity of the Pd(II) centers in **2** as compared to that in **1**. The six Pd–Br bonds can be divided into three different sets with significantly different lengths. As expected, the terminal Pd–Br bonds are the shortest (2.3896(13)–2.4145(13) Å), whereas the bridged bonds that are *trans* to the carbenes are the longest (2.5388(11)–2.5322(11) Å). The latter weak links justify the bridge cleavage of **2** by CH_3CN and DMF. The cleavage of **2** with the two coordinating solvents affords complexes **3** (CH_3CN) and **4** (DMF), respectively, which also have been structurally characterized by single-crystal X-ray diffraction studies. The molecular structures of **3** and **4** are depicted in Figures 4 and 5, respectively.

Both are square-planar mononuclear and monocarbene Pd(II) complexes with a weakly coordinated solvent molecule occupying the position *trans* to the carbene ligand. The Pd–C bond lengths are 1.936(3) and 1.921(2) Å for complexes **3** and **4**, respectively. These Pd–C bond distances are shorter than those in **1**, which again reflects a more Lewis acidic metal center due to the only weakly donating CH_3CN and DMF ligands, respectively. The dihedral angles between carbene ring planes and the PdBr₂CH₃CN or PdBr₂DMF coordination planes amount to 76.5° and 73.8°, respectively. The adjacent *N*-benzyl rings are oriented almost orthogonally to the benzothiazolyl rings with C(1)–N(1)–C(8) angles of 91.2° and 95.3° for complexes **3** and **4**, respectively.

Mizoroki–Heck Catalysis. With the isolation and characterization of this series of N,S-heterocyclic carbenes, we are now able to study and directly compare the catalytic activities between mono- and dicarbene as well as between mono- and dinuclear Pd(II) complexes. The activities of **1–4** toward the Mizoroki–Heck coupling reactions of various aryl bromides and chlorides with *tert*-butyl acrylate yielding the corresponding cinnamates are given in Table 2. All the complexes are air-stable, and hence there is no necessity for glovebox handling. The dicarbene complex **1** is efficient toward coupling between 4-bromobenzaldehyde or 4-bromoacetophenone and the acrylate, giving near-quantitative yields (Table 2, entries 1–6). Moderate yields were obtained when deactivated aryl bromides are used (entries 7–9). To further investigate the effect of the catalyst loading on the conversion rate, we examined the coupling of 4-bromobenzaldehyde with the acrylate. From entries 1–4, the loading of catalyst from 1 mol % to 0.05 mol % gave a quite quantitative conversion.

A kinetic plot of the coupling of the electron-withdrawing 4-bromobenzaldehyde under 1 mol % catalyst **1** is given in Figure 6. The reaction is essentially complete within 3 h (^1H NMR determination), whereas up to 60% of product is formed within the first 20 min. Complex **1** thus promotes a remarkably fast coupling, although the reaction profile shows an induction period for the first 10 min upon mixing. It suggests a fairly rapid reduction of Pd(II) to the catalytically active Pd(0). The sigmoidal turnover points to an initially sluggish product formation followed by a marked increase in turnover with time. A similar activation step has been reported for *cis*-diiodo-bis-(*N,N'*-dimethylbenzimidazolin-2-ylidene)palladium(II).¹⁷ This reductive process can be accomplished by traces of formic acid in DMF.^{10a} When DMF is replaced by, for example, toluene, the conversion decreases markedly to only 18% (entry 5).

The catalytic efficiency of the dinuclear **2** is the poorest among our complexes and unsatisfactory in toluene (entries 10–13), giving the best yield of 47% (entry 11). This could be

(13) Schönherr, H. J.; Wanzlick, H. W. *Chem. Ber.* **1970**, *103*, 1037.

(14) Öfele, K. *J. Organomet. Chem.* **1968**, *12*, p42.

(15) Herrmann, W. A.; Elison, M.; Fisher, J.; Köcher, C.; Artus, G. R. *J. Angew. Chem., Int. Ed. Engl.* **1995**, *34*, 2371.

(16) Herrmann, W. A.; Reisinger, C.-P.; Spiegler, M. *J. Organomet. Chem.* **1998**, *557*, 93.

(17) Huynh, H. V.; Ho, J. H. H.; Neo, T. C.; Koh, L. L. *J. Organomet. Chem.* **2005**, *690*, 3854.

(18) Marschall, C.; Ward, M. F.; Harrison, W. T. A. *Tetrahedron Lett.* **2004**, *45*, 5703.

Table 1. Selected Bond Lengths [Å] and Angles [deg] for Salt **A** and Complexes **1–4**

	A	1	2	3	4
Pd(1)–C(1)		1.971(5)	1.936(7)	1.936(3)	1.921(2)
Pd(1)–C(15)		1.976(4)			
Pd(1)–Br(1)		2.4535(6)	2.4582(13)	2.4234(4)	2.4379(4)
Pd(1)–Br(2)		2.4690(6)	2.5388(11)	2.4476(4)	2.4236(4)
Pd(1)–Br(3)			2.3896(13)		
Pd(1)–N(2)				2.063(3)	
Pd(1)–O(1)					2.1006(18)
Pd(2)–C(15)			1.960(8)		
Pd(2)–Br(1)			2.5322(11)		
Pd(2)–Br(2)			2.4449(13)		
Pd(2)–Br(4)			2.4145(13)		
O(1)–C(15)					1.230(3)
S(1)–C(1)	1.6901(19)	1.713(5)	1.712(8)	1.699(3)	1.710(3)
S(2)–C(15)		1.710(5)	1.709(8)		
N(1)–C(1)	1.314(2)	1.324(6)	1.323(9)	1.330(3)	1.333(3)
N(1)–C(8)	1.483(2)	1.468(6)	1.477(10)	1.467(3)	1.465(3)
N(2)–C(15)		1.327(6)		1.119(4)	1.307(3)
N(2)–C(16)					1.452(3)
N(2)–C(17)					1.434(4)
N(2)–C(22)		1.473(6)			
N(3)–C(15)			1.309(11)		
N(3)–C(22)			1.497(10)		
C(15)–C(16)				1.458(5)	
Br(1)–Pd(1)–Br(2)		91.21(2)	87.10(4)		
Br(2)–Pd(2)–Br(1)			87.54(4)		
Br(3)–Pd(1)–Br(2)			94.17(4)		
Br(4)–Pd(2)–Br(1)			91.79(4)		
C(1)–N(1)–C(8)	123.63(16)	122.7(4)	123.5(7)	123.8(2)	122.6(2)
C(1)–Pd(1)–Br(1)		88.95(13)	92.1(2)	90.15(9)	88.02(7)
C(1)–Pd(1)–Br(2)				88.43(9)	90.68(7)
C(1)–Pd(1)–Br(3)			86.6(2)		
C(1)–Pd(1)–C(15)		89.74(19)			
C(15)–N(2)–C(16)					121.4(3)
C(15)–N(2)–C(17)					120.5(2)
C(15)–N(2)–C(22)		123.0(4)			
C(15)–N(2)–Pd(1)				175.9(3)	
C(15)–N(3)–C(22)			123.9(7)		
C(15)–O(1)–Pd(1)					127.73(19)
C(15)–Pd(1)–Br(2)		90.18(14)			
C(15)–Pd(2)–Br(2)			90.0(3)		
C(15)–Pd(2)–Br(4)			90.7(3)		
C(17)–N(2)–C(16)					118.1(2)
N(1)–C(1)–Pd(1)		129.2(4)	130.0(6)		129.48(19)
N(1)–C(1)–S(1)	114.14(14)	110.9(3)	111.1(5)	111.6(2)	111.31(18)
N(2)–C(15)–C(16)				178.3(5)	
N(2)–C(15)–Pd(1)		131.1(4)			
N(2)–C(15)–S(2)		110.2(3)	111.7(6)		
N(2)–Pd(1)–Br(1)				91.56(9)	
N(2)–Pd(1)–Br(2)				89.88(9)	
N(3)–C(15)–Pd(2)			128.8(6)		
O(1)–C(15)–N(2)					123.8(3)
O(1)–Pd(1)–Br(1)					93.88(5)
O(1)–Pd(1)–Br(2)					87.58(5)
Pd(1)–Br(1)–Pd(2)			92.6(4)		
Pd(2)–Br(2)–Pd(1)			92.76(4)		
S(1)–C(1)–Pd(1)		119.8(3)	118.9(4)	119.97(15)	119.12(13)
S(2)–C(15)–Pd(1)		118.7(2)			
S(2)–C(15)–Pd(21)			119.4(5)		

attributed to its high stability in toluene; the poor donor character of toluene also does not promote the vacant site formation through bridge cleavage. Use of DMF as solvent for **2** effectively gives **4**.

The activities of **3** were examined in three different solvents, viz., CH₃CN, DMF, and toluene (entries 14–24) to compare with compounds **1–2** and **4**. The best activity is observed in DMF, giving 95% yield when 4-bromobenzaldehyde is used (entry 16). In CH₃CN, the highest conversion recorded is 54% (entry 19), with slight improvements when sodium formate is added (entries 15, 19, and 21). The reaction in toluene gives a poor yield of only 19% (entry 17). The higher donor character of DMF appears to provide the best catalyst stability. Accordingly, toluene gives least support to unsaturated species. The

activity of **3** depends significantly on the temperature and solvent. In most cases, decomposition occurs, giving rise to palladium black. These suggest that **3** is unstable under the catalytic conditions, which could explain some poor activities.

The above results suggest some benefits for the use of DMF as a solvent or solvating ligands. Indeed when the DMF complex **4** is used, quantitative yields of 4-bromobenzaldehyde, 4-bromoacetophenone, and 4-bromoanisole are obtained (entries 25–27). However, this does not apply to deactivated aryl bromides such as 4-bromophenol and 4-bromophenylmethanol, which generally see poor conversions (entries 28 and 29).

We have also tested the reactivity of our complexes with activated aryl chlorides and deactivated aryl chlorides such as 4-chlorobenzaldehyde, 4-chloroacetophenone, and 4-chloroben-

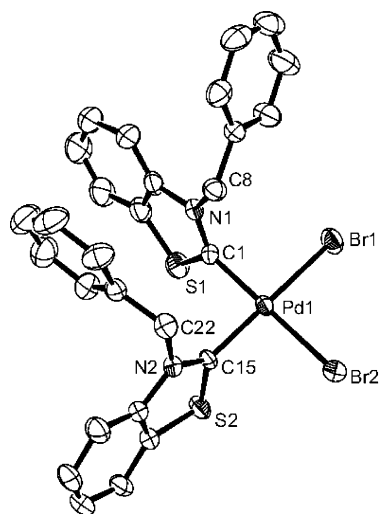


Figure 2. ORTEP view of the molecule $[\text{PdBr}_2(\text{NHC})]$ (**1**) with 50% thermal ellipsoids and labeling scheme.

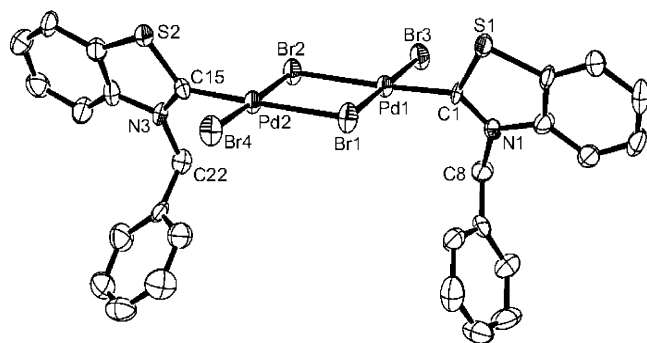


Figure 3. ORTEP view of the molecule $[\text{PdBr}_2(\text{NHC})]_2$ (**2**) with 50% thermal ellipsoids and labeling scheme.

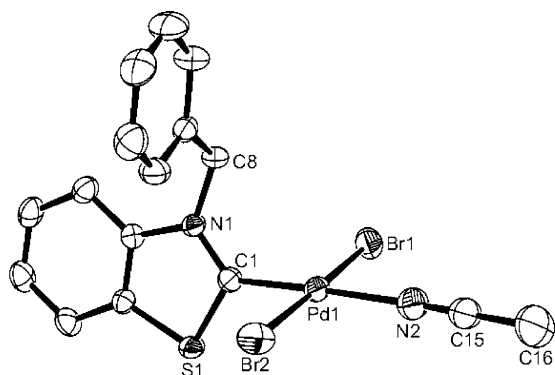


Figure 4. ORTEP view of the molecule $[\text{PdBr}_2(\text{NHC})(\text{CH}_3\text{CN})]$ (**3**) with 50% thermal ellipsoids and labeling scheme.

zonitrile. However, the recorded catalytic activity is quite low (yield below 10% and slightly improved, <20%, when tetrabutylammonium bromide was added) for all catalysts tested under the reaction conditions reported in Table 2. The reactivity of oxalin-2-ylidene palladium complexes also showed quite low yield for the coupling-activated aryl chloride.¹⁹ We presumed that the catalytic effects were brought about by a less electro-negative sulfur as opposed to nitrogen.

Remarkably, complexes **1** and **4** display a greater activity than complexes **2** and **3**. On the whole, the catalytic activities

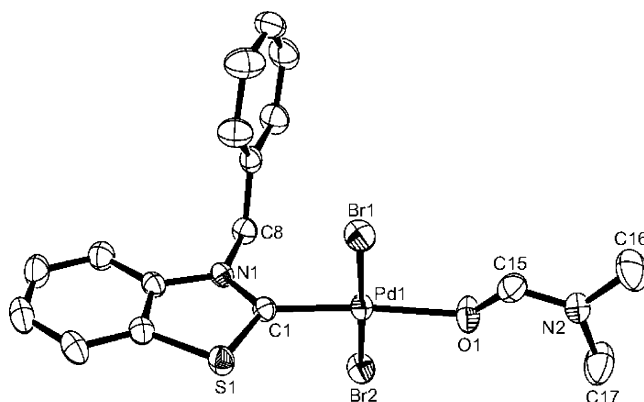


Figure 5. ORTEP view of the molecule $[\text{PdBr}_2(\text{NHC})(\text{DMF})]$ (**4**) with 50% thermal ellipsoids and labeling scheme.

of complexes **1** and **4** are comparable with Caló's bis(2,3-dihydro-3-methylbenzothiazole-2-ylidene)palladium(II) diiodide complex in molten tetrabutylammonium bromide.^{10a}

In conclusion, we have developed a simple, direct method for the synthesis of the *N*-benzylbenzothiazolium salt and the related benzothiazolin-2-ylidene complexes of palladium. The resulting complexes exhibit high catalytic activity in the Heck reaction involving aryl bromides. We are currently extending this synthetic strategy to include other *N*-alkyl or *N*-aryl substituents as well as complexes of other transition metals. Such extended investigations would justify the rich potential of *N,S*-heterocyclic carbenes in systems beyond Heck coupling, especially those that are more receptive to catalysts, which carry carbenes that are less basic.⁹

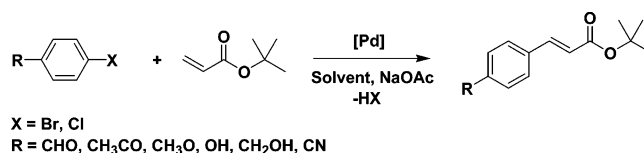
Experimental Section

General Procedures. Unless otherwise stated, all manipulations were performed without taking precautions to exclude air and moisture. All solvents were used as received. Benzothiazole was purchased from Sigma-Aldrich and distilled prior to use. $\text{Pd}(\text{OAc})_2$ was purchased from Sigma-Aldrich and used as received. ^1H and ^{13}C NMR spectra were recorded on Bruker ACF 300 and Bruker AMX 500 spectrometers using Me_4Si as internal standard. ESI mass spectra were obtained using a Finnigan LCQ. The yields of C–C coupling products were determined by using a Finnigan/MAT 95XL-T spectrometer. Elemental analyses were performed on a Perkin-Elmer PE 2400 elemental analyzer at the Department of Chemistry, National University of Singapore. Repeated purification steps did not give satisfactory analytical data for **1** and **3**. They are prone to solvate (and H_2O) entrapment. The latter is also susceptible to loss of the CH_3CN ligand and subsequent dimerization to form **2**.²⁰

***N*-Benzylbenzothiazolium Bromide (A).** A mixture of benzothiazole (3.714 g, 27.5 mmol) and benzyl bromide (4.704 g, 27.5 mmol) was stirred at 60 °C overnight. The off-white solid thus obtained was washed several times with diethyl ether. Diffusion of diethyl ether into a concentrated dichloromethane solution yielded transparent crystals suitable for X-ray diffraction studies. Yield: 8.34 g (27.23 mmol, 99%). ^1H NMR (300.1 MHz, CDCl_3): δ 12.27 (s, 1H, NCH), 8.30 (d, $^3J_{\text{HH}} = 8.04$ Hz, 1H, Ar–H), 8.08 (d, $^3J_{\text{HH}} = 8.43$ Hz, 1H, Ar–H), 7.76 (m, 2H, Ar–H), 7.53 (m, 2H, Ar–H), 7.34 (m, 3H, Ar–H), 6.42 (s, 2H, CH_2). $^{13}\text{C}\{^1\text{H}\}$ NMR (75.5 MHz, CDCl_3): δ 165.1 (NCH), 140.1, 131.5, 131.3, 130.0, 129.5, 129.4, 129.0, 128.3,

(19) Tubora, C.; Biffis, A.; Basato, M.; Benetollo, F.; Cavelli, K. J.; Ooi, L. *Organometallics* **2005**, *24*, 4153.

(20) Huynh, H. V.; Han, Y.; Ho, J. H. H.; Tan, G. K. *Organometallics* **2006**, *25*, 3267.

Table 2. Mizoroki–Heck Coupling Reactions^a Catalyzed by Complexes 1–4

entry	catalyst	catalyst load [mol %]	aryl halide	solvent	t [h]	temp [°C]	yield ^b [%]
1	1	1	4-bromobenzaldehyde	DMF	22	100	100
2	1	0.5	4-bromobenzaldehyde	DMF	22	100	100
3	1	0.25	4-bromobenzaldehyde	DMF	22	100	99
4	1	0.05	4-bromobenzaldehyde	DMF	22	100	95
5	1	1	4-bromobenzaldehyde	toluene	17	100	18
6	1	1	4-bromoacetophenone	DMF	21	110	98
7	1	1	4-bromoanisole	DMF	21	110	79
8	1	1	4-bromophenol	DMF	21	110	75
9	1	1	4-bromophenylmethanol	DMF	21	110	77
10	2	1	4-bromobenzaldehyde	toluene	17	100	17
11	2	1	4-bromoacetophenone	toluene	17	100	47
12	2	1	4-bromoanisole	toluene	17	100	25
13	2	1	4-bromoanisole	toluene ^c	21	110	25
14	3	1	4-bromobenzaldehyde	CH ₃ CN	21	60	10
15	3	1	4-bromobenzaldehyde	CH ₃ CN ^c	21	60	19
16	3	1	4-bromobenzaldehyde	DMF	17	110	95
17	3	1	4-bromobenzaldehyde	toluene	17	100	19
18	3	1	4-bromoacetophenone	CH ₃ CN	21	60	30
19	3	1	4-bromoacetophenone	CH ₃ CN ^c	21	60	54
20	3	1	4-bromoanisole	CH ₃ CN	21	60	29
21	3	1	4-bromoanisole	CH ₃ CN ^c	21	60	30
22	3	1	4-bromoanisole	DMF	17	110	53
23	3	1	4-bromophenol	CH ₃ CN	21	60	7
24	3	1	4-bromophenylmethanol	CH ₃ CN	21	60	32
25	4	1	4-bromobenzaldehyde	DMF	19	110	100
26	4	1	4-bromoacetophenone	DMF	19	110	100
27	4	1	4-bromoanisole	DMF	19	110	99
28	4	1	4-bromophenol	DMF	19	110	16
29	4	1	4-bromophenylmethanol	DMF	19	110	12
30	1	1	4-chlorobenzaldehyde	DMF	42	100	8
31	1	1	4-chloroacetophenone	DMF	42	100	5
32	1	1	4-chlorobenzonitrile	DMF	42	100	5
33	1	1	4-chlorobenzaldehyde	DMF ^d	20	110	8
34	1	1	4-chloroacetophenone	DMF ^d	20	110	5
35	1	1	4-chlorobenzonitrile	DMF ^d	20	110	8
36	4	1	4-chlorobenzaldehyde	DMF	42	100	8
37	4	1	4-chloroacetophenone	DMF	42	100	4
38	4	1	4-chlorobenzonitrile	DMF	42	100	6
39	4	1	4-chlorobenzaldehyde	DMF ^d	20	110	17
40	4	1	4-chloroacetophenone	DMF ^d	20	110	5
41	4	1	4-chlorobenzonitrile	DMF ^d	20	110	10

^a 1 mmol of aryl halide, 1.5 mmol of base, 1.2 mmol of *tert*-butyl acrylate; reaction conditions generally not optimized. ^b Yields were determined by GC/MS. ^c With addition of 1.5 mmol of NaO₂CH. ^d With addition of 1.5 mmol of [N(*n*-C₄H₉)₄]Br.

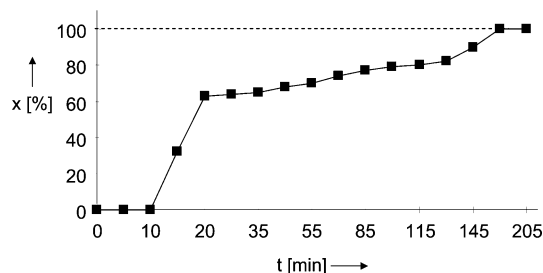


Figure 6. Concentration/time diagram (amount of substance *x* [%], time *t* [min]) for the Mizoroki–Heck olefination of 4-bromobenzaldehyde with *tert*-butyl acrylate to form *tert*-butyl (*E*)-4-formylcinnamate (■) catalyzed by complex 1.

124.8, 117.2 (Ar–C), 56.7 (CH₂). MS (ESI, positive mode) *m/z* (%): 226 (100) [M – Br]⁺. Anal. Calc for C₁₄H₁₂BrNS (M = 306.22): C, 54.91; H, 3.95; N, 4.57; S, 10.47. Found: C, 54.72; H, 3.73; N, 4.48; S, 10.46.

cis-Dibromobis(*N*-benzylbenzothiazolin-2-ylidene)palladium(II) (1). A mixture of A (306 mg, 1 mmol) and Pd(OAc)₂ (112 mg, 0.5 mmol) was suspended in acetonitrile (30 mL) and refluxed overnight. The orange precipitate thus obtained was washed several times with diethyl ether and water. Crystallization from dichloromethane/diethyl ether gave yellow crystalline needles suitable for X-ray diffraction. Yield: 326 mg (0.45 mmol, 91%). ¹H NMR (500 MHz, DMSO-*d*₆): δ 8.12 (d, ³J_{HH} = 7.55 Hz, 2H, Ar–H), 7.53–7.25 (m, 16H, Ar–H), 6.38 (br s, 4H, CH₂). ¹³C{¹H} NMR (125 MHz, DMSO-*d*₆): δ 203.8 (NCH), 142.5, 135.4, 134.6, 129.1, 128.9, 127.7, 127.4, 126.0, 123.2, 116.3 (Ar–C), 58.7 (CH₂). MS (ESI, positive mode) *m/z* (%): 637 (100) [M – Br]⁺. Anal. Calc for C₂₈H₂₂Br₂N₂PdS₂ (M = 716.84): C, 46.92; H, 3.09; N, 3.91; S, 8.94. Found: C, 45.75; H, 3.20; N, 3.97; S, 8.51.

Dibromo(*μ*-dibromo)bis(*N*-benzylbenzothiazolin-2-ylidene)dipalladium(II) (2). A mixture of A (306 mg, 1 mmol) and Pd(OAc)₂ (112 mg, 0.5 mmol) was suspended in DMSO (5 mL) and heated at 70 °C overnight. The solvent was removed under

Table 3. Selected X-ray Crystallographic Data for Salt A and Complexes 1–4

	A	1·0.5CH ₂ Cl ₂ ·0.5H ₂ O	2·CHCl ₃	3	4
formula	C ₁₄ H ₁₂ BrNS	C _{28.5} H ₂₄ Br ₂ ClN ₂ O _{0.5} PdS ₂	C ₂₉ H ₂₃ Br ₄ Cl ₃ N ₂ Pd ₂ S ₂	C ₁₆ H ₁₄ Br ₂ N ₂ PdS	C ₁₇ H ₁₈ Br ₂ N ₂ OPdS
fw	306.22	768.29	1102.40	532.57	564.61
color, habit	colorless, rod	colorless, needle	yellow, block	yellow, thin plate	orange, block
cryst size [mm]	0.60 × 0.20 × 0.10	0.30 × 0.06 × 0.05	0.14 × 0.10 × 0.06	0.20 × 0.12 × 0.04	0.40 × 0.30 × 0.12
temp [K]	223(2)	223(2)	223(2)	223(2)	223(2)
cryst syst	monoclinic	triclinic	triclinic	monoclinic	monoclinic
space group	<i>P</i> 2 ₁ / <i>c</i>	<i>P</i> 1̄	<i>P</i> 1̄	<i>P</i> 2 ₁ / <i>n</i>	<i>P</i> 2 ₁ / <i>n</i>
<i>a</i> [Å]	8.2698(7)	8.4955(4)	9.2077(14)	8.5015(5)	8.8511(8)
<i>b</i> [Å]	12.2681(10)	10.8089(6)	11.6041(18)	11.9451(7)	12.6296(11)
<i>c</i> [Å]	13.0713(11)	16.0904(8)	16.817(3)	17.4372(10)	16.9529(15)
α [deg]	90	87.9840(10)	78.703(3)	90	90
β [deg]	103.714(2)	82.3920(10)	74.761(4)	91.4610(10)	92.234(2)
γ [deg]	90	83.3270(10)	85.044(3)	90	90
<i>V</i> [Å ³]	1288.34(19)	1454.31(13)	1698.9(5)	1770.19(18)	1893.7(3)
<i>Z</i>	4	2	2	4	4
<i>D</i> _c [g cm ⁻³]	1.579	1.754	2.155	1.998	1.980
radiation used	Mo Kα	Mo Kα	Mo Kα	Mo Kα	Mo Kα
μ [mm ⁻¹]	3.328	3.644	6.146	5.677	5.317
θ range [deg]	2.31–27.50	1.90–27.50	2.00–25.00	2.07–27.50	2.01–27.50
no. of unique data	8816	19 112	16 811	12 261	13 220
max., min. transmn	0.7319, 0.2400	0.8388, 0.4077	0.7093, 0.4799	0.8048, 0.3964	0.5679, 0.2249
final <i>R</i> indices [<i>I</i> > 2σ(<i>I</i>)]	<i>R</i> 1 = 0.0266	<i>R</i> 1 = 0.0520	<i>R</i> 1 = 0.0594	<i>R</i> 1 = 0.0298	<i>R</i> 1 = 0.0261
<i>R</i> indices (all data)	<i>wR</i> 2 = 0.0652 <i>R</i> 1 = 0.0329	<i>wR</i> 2 = 0.1154 <i>R</i> 1 = 0.0676	<i>wR</i> 2 = 0.1105 <i>R</i> 1 = 0.0994	<i>wR</i> 2 = 0.0672 <i>R</i> 1 = 0.0406	<i>wR</i> 2 = 0.0618 <i>R</i> 1 = 0.0345
goodness-of-fit on <i>F</i> ²	<i>wR</i> 2 = 0.0676 1.062	<i>wR</i> 2 = 0.1223 1.078	<i>wR</i> 2 = 0.1230 1.068	<i>wR</i> 2 = 0.0710 1.028	<i>wR</i> 2 = 0.0643 1.015
peak/hole [e Å ⁻³]	0.431/–0.273	1.127/–0.792	1.042/–0.710	0.744/–0.332	0.629/–0.342

vacuum, and chloroform (10 mL) was added. The mixture was left to stand for 2 days. The orange solid thus obtained was filtered, washed with small amounts of chloroform and diethyl ether, and dried under vacuum. X-ray-quality crystals were obtained from a saturated CHCl₃ solution. Yield: 109 mg (0.11 mmol, 45%). ¹H NMR (300.1 MHz, DMSO-*d*₆): δ 8.15 (br s, 2H, Ar–H), 7.70–7.29 (m, 16H, Ar–H), 6.50 (s, 4H, CH₂). ¹³C{¹H} NMR (75.5 MHz, DMSO-*d*₆): δ 142.2, 136.0, 134.3, 129.1, 128.7, 128.0, 127.5, 125.9, 123.1, 115.8 (Ar–C), 58.9 (CH₂). The signal for the carbene carbon could not be detected under the given conditions. MS (FAB) *m/z* (%): 903 (100) [M – Br]⁺. Anal. Calc for solvate Pd₂Br₄(C₁₄H₉NS)₂·CHCl₃ (M = 1102.45): C, 31.59; H, 2.10; N, 2.54; S, 5.82. Found: C, 31.59; H, 2.32; N, 2.76; S, 6.09.

trans-Dibromo(acetonitrile)(*N*-benzylbenzothiazolin-2-ylidene)palladium(II) (3). Acetonitrile (15 mL) was added to complex 2 (295 mg, 0.3 mmol) and the mixture heated under reflux overnight. The clear yellow solution was cooled to ambient temperature and the solvent evaporated under vacuum. Yellow cubic single crystals of 3 were obtained from a concentrated acetonitrile/diethyl ether solution upon standing. Yield: 295 mg (0.55 mmol, 92%) was obtained. ¹H NMR (300.1 MHz, CDCl₃): δ 7.80 (m, 1H, Ar–H), 7.50–7.34 (m, 8H, Ar–H), 6.46 (br s, 2H, CH₂), 2.00 (s, 3H, CH₃CN). ¹³C{¹H} NMR (75.5 MHz, CDCl₃): δ 191.5 (NCS), 142.2, 136.4, 133.0, 129.2, 129.1, 128.8, 127.4, 127.2, 125.6, 121.9 (Ar–C), 115.1 (CH₃CN), 59.7 (CH₂), 1.78 (CH₃CN). MS (FAB) *m/z* (%): 572 (18) [M + K]⁺. Anal. Calc for C₁₆H₁₄Br₂N₂PdS (M = 532.58): C, 36.08; H, 2.65; N, 5.26; S, 6.02. Found: C, 33.52; H, 3.00; N, 5.33; S, 6.16.

trans-Dibromo(*N*-benzylbenzothiazolin-2-ylidene)(*N,N*-dimethylformamide)palladium(II) (4). A solution of complex 2 (295 mg, 0.3 mmol) in *N,N*-dimethylformamide (15 mL) was heated at 80 °C overnight. The yellow solution thus obtained was cooled to ambient temperature and filtered, and the solvent

of the filtrate was removed under vacuum. Diffusion of diethyl ether into a concentrated DMF solution afforded yellow cubic crystals of 5 suitable for X-ray diffraction studies. Yield: 288 mg (0.51 mmol, 85%) was obtained. ¹H NMR (300.1 MHz, CDCl₃): δ 8.02 (s, 1H, CHO), 7.82 (d, ³*J*_{HH} = 6.72 Hz, 2H, Ar–H), 7.52–7.30 (m, 7H, Ar–H), 6.51 (br s, 2H, CH₂), 2.96 (s, 3H, CH₃), 2.88 (s, 3H, CH₃). ¹³C{¹H} NMR (75.5 MHz, CDCl₃): δ 191.9 (NCS), 162.6 (CHO), 142.5, 136.4, 133.0, 129.3, 128.8, 127.5, 127.2, 125.6, 121.9, 115.2 (Ar–C), 59.9 (CH₂), 36.5 (CH₃), 31.5 (CH₃). MS (FAB) *m/z* (%): 412 (40) [M – Br – DMF]⁺. Anal. Calc for C₁₇H₁₈Br₂N₂OPdS (M = 564.63): C, 36.16; H, 3.21; N, 4.96; S, 5.68. Found: C, 36.43; H, 3.25; N, 5.15; S, 5.83.

General Procedure for the Heck Reaction. NaOAc (1.5 mmol), aryl halide (1 mmol), and *tert*-butyl acrylate (1.2 mmol) were placed in a reaction flask equipped with a stirring bar. DMF (3 mL) was introduced, and the resulting suspension was heated to 100 °C for 10 min before the catalyst was added. After the desired reaction time, the reaction mixture was cooled to ambient temperature. Water was added, and the aqueous phase was extracted with dichloromethane (3 × 4 mL). The combined organic phases were dried over MgSO₄ and filtered, and the solution was analyzed by GC/MS.

X-ray Diffraction Studies. Suitable crystals were mounted on quartz fibers and X-ray data collected on a Bruker AXS APEX diffractometer, equipped with a CCD detector, using graphite-monochromated Mo Kα radiation (λ = 0.71073 Å). The data were corrected for Lorentz and polarization effects with the SMART suite programs²¹ and for absorption effects with SADABS.²² Structure solution and refinement were carried

(21) SMART version 5.1; Bruker Analytical X-ray Systems: Madison, WI, 2000.

(22) Sheldrick, G. M. SADABS: A Program for Empirical Absorption Correction; Göttingen, Germany 2001.

out with the SHELXTL suite of programs.²³ The structures were solved by direct methods to locate the heavy atoms, followed by difference maps for the light non-hydrogen atoms. Selected crystal data for salt **A** and complexes **1–4** are summarized in Table 3.

Acknowledgment. We thank the National University of Singapore (NUS) for financial support and the reviewers for

(23) *SHELXTL* version 6.10; Bruker Analytical X-ray Systems: Karlsruhe, 2000.

some useful comments. Technical support from staff at the CMMAC of NUS is appreciated. H.V.H. is grateful to the Alexander von Humboldt Foundation for a Feodor Lynen Research Fellowship. S.K.Y. thanks NUS for the research scholarship.

Supporting Information Available: Crystallographic data for **A** and **1–4** in CIF format. This material is available free of charge via the Internet at <http://pubs.acs.org>.

OM060510N